Development of Visible-Light Active TiO_2 and Activated Carbon Fiber Composites in Single Step

C.-Y. Tsai*, H.-C. Hsi** and K.-S. Fan***

*Department of Safety, Health and Environment Engineering, National Kaohsiung First University of Science and Technology, 2, Juoyue Rd., Kaohsiung 811, Taiwan, u9315918@ccms.nkfust.edu.tw
**Institute of Environmental Engineering and Management, National Taipei University of Technology, 1, Sec. 3, Chung-hsiao E. Rd., Taipei 106, Taiwan, hchsi@ntut.edu.tw
***Department of Safety, Health and Environment Engineering, National Kaohsiung First University of Science and Technology, 2, Juoyue Rd., Kaohsiung 811, Taiwan, ksfan@ccms.nkfust.edu.tw

ABSTRACT

The aim of this study is to develop visible-light photocatalyst nanopowders by N_2 modified TiO_2 matrix via gas-phase evaporation condensation. The formed visible-light TiO_2 nanopowders are subsequently doped onto the surface of activated carbon fiber (ACF). This TiO_2/ACF composite possesses the capability of adsorption, concentration, and photodestruction of gaseous contaminants. The formed TiO_2 nanopowders and TiO_2/ACF composites were characterized with TEM, XRD, UV-Vis and ESEM. The obtained results indicated that the nanopowders had a size within 10 – 40 nm. The formed TiO_2 nanopowders were a mixture of anatase and rutile. The TiO_2 with N_2 modified has an evident red-shift in wavelength absorption. ESEM results also showed that the synthesized TiO_2 nanopowders were uniformly distributed on the ACF surface. These results revealed that the proposed thermal plasma condensation method successfully fabricated visible-light TiO_2 /ACF in a single step.

Keywords: N_2 modified TiO_2, activated carbon fiber, evaporation condensation, thermal plasma

1 INTRODUCTION

Titanium dioxide (TiO_2) is a commonly used photocatalyst due to its chemical stability. Nevertheless, the manufacturing process of TiO_2 strongly influences the purity and physical properties of resulting nanoparticles. These properties subsequently affect the characteristics of TiO_2 photocatalytic reactions. One crucial defect of TiO_2 is that its band gap energy of 3.2 eV to make the TiO_2 only being excited by UV light. Therefore, significant changes have been studied to modify TiO_2. A proficient way is to extend the absorbance of TiO_2 to visible light. Recently, many literatures have described that substitution doping with nitrogen atom in TiO_2 lattice shifts the absorption edge to lower energies through band gap narrowing, because the related impurity states are supposed to be close to the valence band maximum [1-3]. Asahi et al. produced theoretical compute for substitution of O_2 in TiO_2 lattice with several anionic materials and showed that the substitute doping of N is the most efficient way for getting the visible light activity of TiO_2 photocatalysis [1]. On the other hand, Yamada et al. synthesized visible-light active TiO_2 particles of which the surface was doped with nitrogen. They sintered a film of the particles on the surface of a glass substrate by spin-casting of TiO_2 sol. Then the film was treated with argon and nitrogen plasma [3].

However, the effectiveness of TiO_2 photocatalyst on destructing contaminants has shown to be largely influenced by the types and concentration of pollutants. The concentration of organic pollutants around TiO_2 has a great effect on decomposition rate. To achieve the goal of completely decomposing targeting pollutants, it is important to increase the interface concentrations of the contaminants for the photocatalytic reactions. Moreover, mineralization of organic pollutants is a result of continuous photocatalysis process, and many intermediate species with higher toxicity are formed during organic pollutant decomposition. Therefore, composites with titanium dioxide as photocatalyst and with large surface would be of great significance. Usually the pollutants concentrated on the support materials migrate to the surface of TiO_2 by diffusion and then get decomposed. But the degradation efficiency of pollutant decreases because of the mass transfer limitation [4]. To ensure an efficient reaction and maximum activity in heterogeneous catalysis, the active phase on the catalyst surface must be highly dispersed over a large specific surface area. To achieve this objective, TiO_2 photocatalyst active species are usually deposited on the surface of highly porous support substrates, such as activated carbon fibers [5-7].

Much recent work was focused on the preparation as well as on the TiO_2/ACF composites. Herbig et al. produced carbon fibers with TiO_2 by liquid phase deposition (LPD). Comparative measurements suggest that the surface specific photocatalytic activity of LPD-derived TiO_2 is higher than that of commercially available P-25 [5]. Liu et al. prepared TiO_2/ACF by sol-gel method. [6]. Zhang et al. prepared Fe_2O_3-TiO_2 coating supported on ACF by a convenient and efficient methodof metal organic chemical vapor deposition. The pore structure of ACF was preserved well after loading with Fe_2O_3-TiO_2 coatings, and exhibited

good photocatalytic activities for the degradation of methyl orange under visible light irradiation [7].

However, so far only a few reports studied preparation methods for TiO_2/ACF composites. Synthetic routes for TiO_2/ACF are usually based on sol-gel method, thus a multi-step synthetic process was needed. Few studies have shown to produce TiO_2/ACF in single step. This study aimed at preparing visible-light TiO_2 nanopowders by nitrogen modified. And let the TiO_2 impacted the ACF at the same time. We considered this single-step process as a potential method to produce high-quality nanoscale visible-light TiO_2/ACF with clean surface and narrow particle size distribution.

2 EXPERIMENTAL

Visible-light TiO_2/ACF composites were synthesized with evaporation condensation method as shown in Fig. 1. Transferred DC plasma torch assembled by Taiwan Plasma Corp. (Kaohsiung, Taiwan) was used as a heating source. The torch electrode that manufactured with copper alloy was cooled by water. Titanium metal of 99.8% purity was used as the evaporation material. Desired power level was maintained by controlling the flow rate of the plasma gases and plasma current. A mixture of nitrogen, argon and helium were used as plasma gas. The flow rate of Ar + He was constant at 2 L min^{-1} varying the concentration of N_2 to control the ration N_2/(Ar + He) from 0, 5, 7 and 10% by volume. The reactor base pressure was 20 kPa. O_2 was used both as a reacting gas and as shelter gas of plasma torch (2 L min^{-1}). The operating current of 110A was considered optimum. The distance between the torch and ACF was 150 mm and the angle of both was 180°. A vacuum pump was connected at the back of reactor which compelled the TiO_2 impact on the ACF.

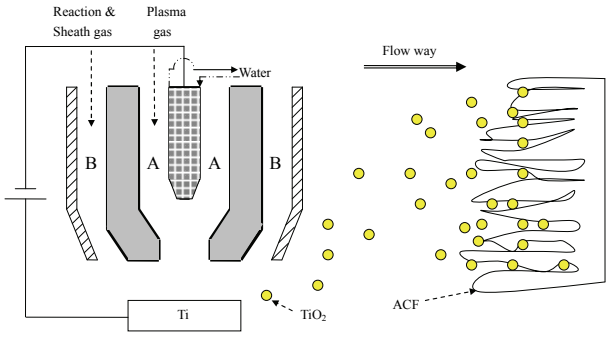

Figure 1: Schematic diagram of transferred DC plasma torch for producing visible-light TiO_2 /ACF composites.

Morphologies and particle sizes of the powders were investigated by transmission electron microscopy (TEM, PHILIPS model CM-200 TWIN). The crystal structure of TiO_2 was evaluated by X-ray diffraction (XRD, SHIMADZU model XRD-600). The diffuse reflectance UV-visible spectra of the TiO_2 photocatalysts were measured using a spectrophotometer (UV-Visible, HITACHI model U3010). The images of TiO_2/ACF and uncovered ACF were observed by environmental scanning electron microscope (ESEM, FEI Quanta model 400 F).

3 RESULTS AND DISCUSSION

3.1 Structural of N_2 Modified TiO_2

The morphology of the nanoparticles was observed with TEM as shown in Fig. 2. The darker areas in the TEM micrographs indicate TiO_2 gathers. In situ nanoparticles in Fig. 2a was well distributed with a diameter of approximately 10 nm. The particle size of each sample was approximately the same. The nano sized particles can be either round or spherical shaped, forming from direct titanium vapors or high agglomeration of primary TiO_2 nanoparticles. When the N_2 was added, it had a little effect on the shape and size of the particles. The average diameter of the nanoparticle increased from 10 to 40 nm when N_2 was added to plasma gas. In contrast, TiO_2 particles in the sample prepared by a 0% N_2 process were smaller and more dispersed than that prepared by a N_2 added process. The aforementioned observations were somewhat expected because the flame temperature of transferred plasma torch was markedly influenced by the types of plasma gases and the magnitudes of applied plasma power. When the N_2 was added to plasma gas, the voltage of plasma was observed to increase from 20.7 to 23.68. The titanium metal, playing a role as the anode in this study, vaporized faster at a higher flame temperature, which caused a quicker and more effective collision between vaporized Ti atoms and oxygen to form TiO_2. As a result, a rapid nucleus growth occurred, which greatly increased the size of the formed nanoparticles. Ramasamy and Selvarajan have reported the increase in the temperature of plasma jet and growth in powder size when N_2 was added. [8]. These results indicated that evaporation condensation process could result in TiO_2 with a more perfect nanoparticle size.

Fig. 3 shows the XRD patterns of the powders as a function of nitrogen concentration ration in nitrogen/(argon + helium) gas mixture. The TiO_2 nanoparticles exhibit well-crystallized anatase phase with (101) preferred orientation and weak bands for rutile phase in the XRD patterns. As shown in Fig 3a, the peaks at 25.3, 37.8, 48.0, 53.8, 54.9 and 62.5° are the diffractions of the (101), (004), (200), (105), (211) and (204) planes of anatase, respectively. Although the peak (2 theta = 27.45 °) of rutile TiO_2 (110) was also observed in the pattern of Fig 3a, it was weak enough to be ignored here. The patterns of the Fig 3b, 3c and 3d particles became broader gradually in the (004) and (200) of anatase as the nitrogen concentration was increased gradually. While nitrogen (5% and 7%) added to plasma gas, the peak of rutile (110) was complete and also observed that anatase transform rutile from peaks at 53.8 and 54.9°. The anatase of TiO_2 transforms into rutile by increase in temperature. Accompanying with the results

obtained from the TEM analyses, it appeared that the nitrogen increased plasma temperature in the formed TiO_2 may promote particles growth. The compounds of Cu were observed to melt from the plasma torch and mixed with the TiO_2 nanopowders when 10% N_2 was added to the plasma gas. In contrast, the pattern of powder as in Fig. 3d was much different in peak broadening and relative peak intensities compared with Fig. 3b, and an additional peak of 2 theta = 36.0°. From the JCPDS database, the d-specing of rutile (101) and Cu_2O (111) is 2.49 and 2.47, respectively. Therefore, the peak primary Cu_2O phase with a minor amount of rutile phase was maintained. The formation of compounds of Cu phase could be explained by the fact that at high plasma temperature, certain percentage of the Cu compounds were present from the plasma torch. Wong et al. indicated that the excess N_2 fraction created TiN, which increased the nitrogen incorporation and destroyed the anatase TiO_2 phase in the TiO_xN_y nanoparticles [9]. XRD results in our study show that the nitrogen supply would influence the composition and crystallinity of the TiO_2 powders. In this study, the nitrogen addition amount is not enough to create TiN.

The data in figure 4 correspond to UV-visible spectra of the nanoparticles synthesized N_2 modified TiO_2 at various nitrogen concentrations and commercial Degussa P-25 TiO_2 over the wavelength range of 300 – 800 nm. In contrast, the nanoparticles of TiO_2 without N_2 supply showed the absorption edge at 390 nm corresponding to the band gap of TiO_2 at 3.18 eV. This result is similar to commercial Degussa P-25 TiO_2. In contrast, the N_2 modified TiO_2 powders showed a strong absorption in the visible range. For the 0%, 5% and 7% nitrogen modified TiO_2 nanoparticles, the absorption edge shifts towards the visible light regions depending on the amount of nitrogen concentration ration in the plasma gas mixture. Significant red shift of the absorption edges to the visible-light region was observed in the 7% N_2 added to plasma gas. As the N_2 concentration was 7%, the absorption edges of the TiO_2 nanoparticles showed red shift at around 490 and 590 nm. We attributed this new absorption band to N atoms modified TiO_2 nanoparticles. This conclusion was based on the following reasons. By comparing the spectra of N_2 modified TiO_2 sample with non-N_2 modified TiO_2, we can conclude that N modification led to the appearance of visible adsorption of TiO_2. The reflection spectrum of modified sample with N_2 shifted to shorter wavelength than that of commercial anatase TiO_2 probably because of a size quantization effect. However, the TEM results can manifest the particle size of N_2 modified TiO_2 larger than non-N_2 TiO_2. The spectrum of 10% N_2 modified TiO_2 was good agreement with the produced new band at around 425 nm. Although, the band gap of 10% N_2 modified TiO_2 at 2.91 was lower than non-N_2 TiO_2 band gap at 3.18 eV. Nonetheless, the absorption edges of 10% N_2 modified TiO_2 had still smaller contrast with 7% N_2 modified TiO_2. XRD results showed presence of the compounds of Cu in TiO_2 powders, hence reduced absorption edges. The foregoing results indicated that 7% N_2 modified TiO_2 nanoparticles belonged to anatase and rutile mixed TiO_2 and had the absorption edge in visible-light.

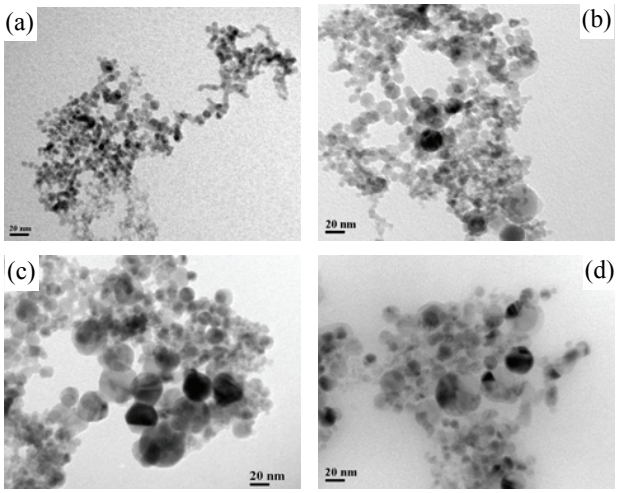

Figure 2: TEM images of TiO_2 nanoparticles synthesized with N_2 added different volume (a)0%, (b)5%, (c)7% and (d)10% to plasma gas.

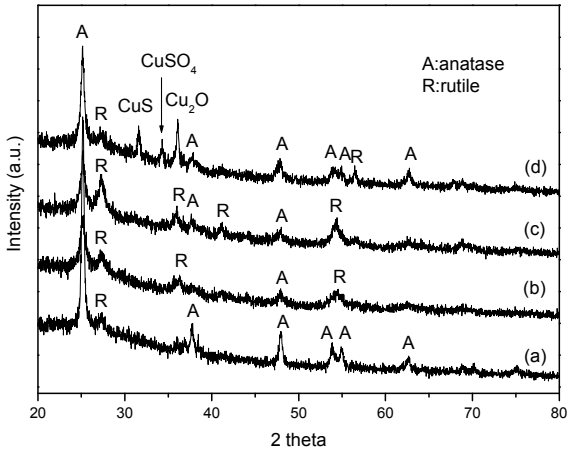

Figure 3: Comparison of the XRD patterns of (a) 0% nitrogen modified TiO_2 nanoparticles, (b) 5%, (c) 7% and (d) 10% nitrogen modified TiO_2 nanoparticles.

3.2 TiO_2/ACF Composites Characterization

Fig. 5 shows the surface morphology of pristine ACF and 7% N_2 modified TiO_2/ACF composites measured by ESEM. Fig 5a shows ESEM analysis of surfaces of pristine ACF. The surface of pristine ACF is full of long shallow grooves. The TiO_2 nanoparticles appeared even and uniform on almost every fiber of ACF as shown in Fig. 5b. From the ESEM photographs, it could be seen that the surface of ACF was not completely covered with the TiO_2

coating. The TiO_2/ACF system retained the same tridimensional shape and almost the same diameter as uncovered ACF. It was deduced the deposited TiO_2 nanoparticles on ACF would have close unprocessed, which was favorable for adsorption and photocatalysis of pollutants.

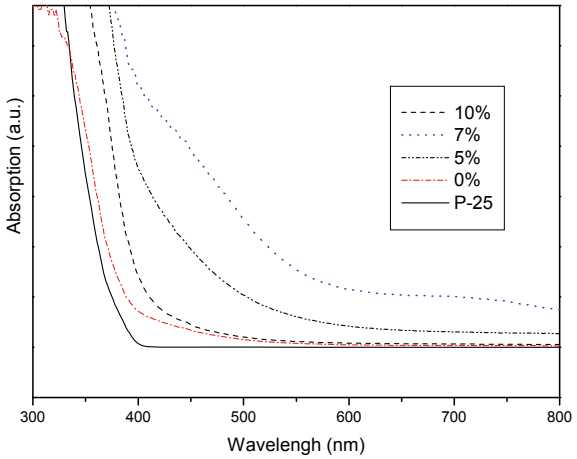

Figure 4: UV-Visible absorption spectra of the P-25, non-N_2 and different concentration N_2 modified TiO_2.

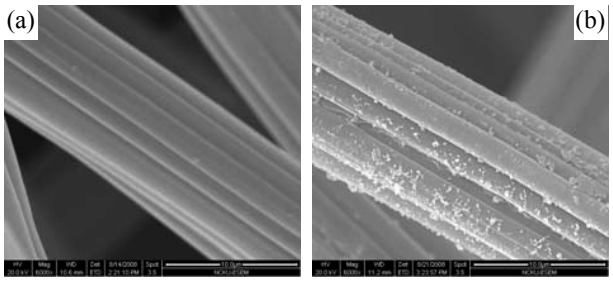

Figure 5: The ESEM surface analysis of samples (a) The blank ACF and (b) TiO_2/ACF composites.

4 CONCLUSION

There are two major difficulties in the TiO_2 gas-solid photocatalytic system: effective immobilization of the TiO_2 particles; and improving the catalytic activity under visible light. To simultaneously solve these two problems, N_2 modified TiO_2 coatings supported on activated carbon fiber, have been prepared in one step by evaporation condensation using a thermal plasma system. Results indicated that the nanoparticles had a size within 10 nm in non-nitrogen environment. The nitrogen added to plasma gas increased the particle size to 10 – 40 nm. The crystal phases of the N_2 modified TiO_2 nanoparticles were mainly in anatase and rutile forms. The TiO_2 nanoparticles exhibit well-crystallized anatase phase and weak band for rutile phase in non-nitrogen plasma gas. The substitution of nitrogen was found to cause a significant red shift in the absorption edge to lower energy due to band gap narrowing. The micropore structure and high specific surface area of ACF were not damaged by deposition of N_2 modified TiO_2. The pore structure of ACF was preserved well after loading with visible-light TiO_2 nanoparticles coatings, so the adsorption ability of ACF was expected to be maintained. These results demonstrated that the proposed thermal plasma method evaporation condensation successfully fabricated visible-light TiO_2 /ACF composites in a single step.

ACKNOWLEDGMENT

This work was supported by National Council of Taiwan (NSC 97-2622-E-327-001-CC3) and Taiwan Plasma Corp., Kaohsiung, Taiwan.

REFERENCES

[1] R. Asahi, T. Morikawa, T. Ohwaki, K. Aoki, and Y. Taga, "Visible-light photocatalysis in nitrogen-doped titanium oxides," Science, 293, 269-271, 2001.

[2] Y. Suda, H. Kawasaki, T. Ueda, and T. Ohshima, "Preparation of high quality nitrogen doped TiO_2 thin film as a photocatalyst using a pulsed laser deposition method," Thin Solid Films, 453-454, 162-166, 2004.

[3] K. Yamada, H. Nakamura, S. Matsushima, H. Yamane, T. Haishi, K. Ohira, and K. Kumada, "Preparation of N-doped TiO_2 particles by plasma surface modification," Comptes rendus - Chimie, 9, 788-793, 2006.

[4] X. W. Zhang, M. H. Zhou, and L. Lei, "Preparation of photocatalytic TiO_2 coatings of nanosized particles on activated carbon by AP-MOCVD," Carbon, 43, 1700-1708, 2005.

[5] B. Herbig and P. Lobmann, "TiO_2 photocatalysts deposited on fiber substrates by liquid phase deposition," Journal of Photochemistry and Photobiology a-Chemistry, 163, 359-365, 2004.

[6] H. H. Liu, R. Yang, and S. M. Li, "Preparation and application of efficient TiO_2/ACFs photocatalyst," Journal of Environmental Sciences-China, 18, 979-982, 2006.

[7] X. W. Zhang and L. C. Lei, "Preparation of photocatalytic Fe_2O_3-TiO_2 coatings in one step by metal organic chemical vapor deposition," Applied Surface Science, 254, 2406-2412, 2008.

[8] R. Ramasamy and V. Selvarajan, "Heat transfer to a single particle injected into a thermal plasma," Computational Materials Science, 15, 265-274, 1999.

[9] M.-S. Wong, H. Pang Chou, and T.-S. Yang, "Reactively sputtered N-doped titanium oxide films as visible-light photocatalyst," Thin Solid Films, 494, 244-249, 2006.